

Original article

## Firing techniques of black slipped pottery from Nepal (12th–3rd century B.C.): The role of Mössbauer spectroscopy

Paola Ricciardi <sup>a,b</sup>, Luca Nodari <sup>c,\*</sup>, Sabrina Gualtieri <sup>a</sup>, Daniela De Simone <sup>d</sup>,  
Bruno Fabbri <sup>a</sup>, Umberto Russo <sup>c</sup>

<sup>a</sup> CNR-ISTEC, Istituto di Scienza e Tecnologia dei Materiali Ceramici, via Granarolo 64, 48018 Faenza (Ra), Italy

<sup>b</sup> Dipartimento di Chimica, Università degli Studi di Firenze, via della Lastruccia 3, 50019 Sesto Fiorentino (FI), Italy

<sup>c</sup> Dipartimento di Scienze Chimiche, Università di Padova and INSTM, UdR Padova, via Marzolo 1, 35131 Padova, Italy

<sup>d</sup> Italian Archaeological Mission to Nepal, ISIAO—Università degli Studi di Napoli ‘L’Orientale’, Napoli, Italy

Received 7 June 2007; accepted 4 December 2007

---

### Abstract

Previously published results have preliminarily characterised the prehistoric production (12th–3rd century B.C.) of black slipped pottery recovered from the excavations of Gotihawa, in Kapilbastu District in Southern Nepal. Some clayey materials, still used nowadays by local potters for producing vessels, have been collected in the surroundings of the site and analysed. Two different ceramic classes have been particularly investigated: the so-called Black Slipped Ware (BSW) and the Northern Black Polished Ware (NBPW). So far it has not been possible to define clearly distinctive markers of these on the basis of either archaeological studies or archaeometric analyses. The main result obtained for the NBPW and BSW pastes is the high compatibility with the examined clays. The use of local clays for artefacts manufacturing is therefore assured. More interesting information is obtained by analysing the glossy layers of the two classes. Three groups of glosses have been evidenced in which the differences are related to the different amounts of potassium, iron and aluminium oxides. The glosses of the Al-group present values of aluminium higher than the corresponding pastes; in the AlFe-group glosses the quantities of aluminium and iron are very high, and finally in the third group (KAlFe) all three elements are more abundant than in the pastes. Practically all the BSW glosses fall in the AlFe group, while the NBPW glosses are distributed in the three groups. Other information regarding working techniques, in particular the firing conditions of the artefacts, have to be clarified in order to assess the whole manufacturing process. The detailed reconstruction of the firing techniques of such artefacts with the usual analytical methodologies (XRF, XRD and observation in thin section) is highly problematic due to the peculiar features of the samples. The low calcium content gives rise to an extremely simple mineralogical composition, without any of the calcium silicates which usually form during firing, and give indications on the firing temperature. Moreover, the absence of crystalline iron oxides in the diffractograms limits the possibility to evaluate the firing temperature to the sole estimate of illite content. The determination of the firing atmosphere is mainly based on a visual examination of the colour of the sample pastes and slips. In an attempt to better define the range of firing temperatures, we have chosen to use Mössbauer spectroscopy on the basis of the high content of iron of the samples. In fact, <sup>57</sup>Fe Mössbauer spectroscopy allows the identification of mineral phases to be used as a “mineralogical thermometer”, such as spinel phases, hercynite and metallic iron. Also, the calculation of the reduction index ( $\text{Fe}^{2+}/\text{Fe}_{\text{TOT}}$ ) yields interesting information regarding the firing technology, and particularly the control of the firing atmosphere by the potter. These results seem to be possibly linked to previous data obtained from the EDS chemical analyses of the above-mentioned three groups of slips.

© 2008 Published by Elsevier Masson SAS.

**Keywords:** Mössbauer spectroscopy; Firing technology; Reduction index; Black slipped pottery; Nepal

---

\* Corresponding author. Tel.: +39 049 827 5321; fax: +39 049 827 5161.

E-mail addresses: [paola.ricciardi@gmail.com](mailto:paola.ricciardi@gmail.com) (P. Ricciardi), [luca.nodari@unipd.it](mailto:luca.nodari@unipd.it) (L. Nodari), [sgualtieri@istec.cnr.it](mailto:sgualtieri@istec.cnr.it) (S. Gualtieri), [desimonedaniela@yahoo.it](mailto:desimonedaniela@yahoo.it) (D. De Simone), [fabbri@istec.cnr.it](mailto:fabbri@istec.cnr.it) (B. Fabbri), [umberto.russo@unipd.it](mailto:umberto.russo@unipd.it) (U. Russo).

## 1. Introduction

### 1.1. Research aims

Mössbauer spectroscopy can certainly not be included among routine methodologies for the archaeometric analysis of pottery finds; nonetheless it has often proved to have the right features to give answers to the questions posed by archaeologists, in such cases where the most commonly used techniques have not yielded satisfactory results [1–6]. Our intention is to point out that Mössbauer spectroscopy has certainly been useful in our analysis of Nepalese black slipped artefacts.

It may not be redundant to underline the importance that pottery has within archaeological research, as a largely spread witness of material culture, and also as a dating object in an excavation context. Besides this, pottery is the product of a variegated and often complex technological process which, when reconstructed, gives interesting indications about the technical, economic, social and cultural features of the society producing the artefact. The characteristics of the firing technique are strongly correlated with the technological level attained in the production. Among them, the most significant and the most frequently investigated in archaeometric research are the maximum temperature reached during firing and the atmosphere (oxidising, semi-reducing or reducing) in which the firing took place [7]. It is also possible to evaluate the variations of temperature within the kiln, the soaking time, the thermal gradient and the total duration of the firing cycle, as demonstrated by Livingstone Smith [8] and Wolf [9] among others.

Several methods have so far been used for the evaluation of the firing technique of ancient pottery [10–14], comprising mostly those yielding the mineral composition of the sample (XRD, thermal analyses, FT-IR), which is in turn an indicator of the reactions which took place during firing, related to both the temperature and the atmosphere.

### 1.2. Archaeological context

The Italian Archaeological Mission to Nepal is a joint research project of the Istituto Italiano per l’Africa e l’Oriente (IsIAO) and the Università degli Studi di Napoli “L’Orientale”. The work of the Italian mission has been focused on Tarai, Nepal’s southernmost land strip [15,16]. The archaeological site of Gotihawa is located along the Indian border, and it has shown a stratigraphic sequence starting at the end of the II millennium B.C. The site is centred around a brick stūpa and a votive pillar, both Buddhist religious monuments dating to the Ashokan period (half of the 3rd century B.C.); the pottery included in this study belongs to the pre-stūpa layers (12th–3rd century B.C.). A few thousand pottery fragments have been recovered during the excavations in the area; archaeologists have classified them into seven groups [17], samples of all of which have been preliminarily analysed by archaeometric techniques. Classes have been identified on the basis of the colour of the paste, the colour of the inner and outer surfaces, the presence of paint, the fabric, the presence, frequency and dimensions of inclusions (distinguishing between organic and inorganic) in

the paste, tactile assessment of the surface, the presence of impressed, incised or painted decoration, and the thickness of the walls. It is worth noting that in many cases, the body and surface colour does not perfectly fit into the classification scheme. The firing took probably place in a stack kiln, following a procedure which may not have differed much from those still in use for black slipped pottery production in the Nepalese area.

## 2. Materials and methods

### 2.1. Materials

Our present work focuses on samples belonging to two ceramic classes, namely the Black Slipped Ware (BSW, six samples) and the Northern Black Polished Ware (NBPW, nine samples). The BSW is the most ancient of the two classes, attested at Gotihawa between the 12th and the 4th century B.C. The BSW samples, all tableware, have a light grey core and surface; they are usually wheel-made, well fired, and have a lustrous and rather thick black slip, which sometimes peels off. The NBPW represents the result of the technological upgrading of the BSW, and is present at Gotihawa between the 9th and the 3rd century B.C. Within this class, it has been possible to identify “proto-NBPW” samples, with thin slips and fairly thick walls, black sections and lustrous black surfaces with red spots. This seems to be an experimental stage in the production of NBPW; its appearance is very similar to BSW, and this leads to difficulties in readily distinguishing the two types. “Real” NBPW, on the other hand, has black, lustrous and burnished surfaces, black and thin slips, black sections and very thin walls (due to the use of a very fast wheel). Lastly, “late NBPW” is not a homogeneous class. The majority of the pot sherds have a bluish-black or greyish black surface, while the others exhibit different colours, varying from light cream to deep brown. Many pot sherds are of the bi-chrome variety; walls vary from very thin to somewhat thick, but all are glossy.

In addition to the pottery, three local clays have been analysed, in order to test their compatibility with the artefacts.

### 2.2. Experimental techniques

Chemical and mineralogical compositions of pastes and clays had been obtained by means of X-ray fluorescence (XRF) and X-ray diffraction (XRD), respectively. Information about the microstructure of pastes and slip layers had been obtained by observations with optical microscopy on thin section and scanning electron microscopy associated with microprobe (SEM-EDS), that gave also the chemical composition of the slip layers. More details about the analytical procedures can be found in the works of Camarda et al. [18,19].

Room Temperature (RT) Mössbauer spectroscopy was performed in a transmission geometry (TMS) in a conventional constant-acceleration spectrometer, using a room temperature Rh matrix  $^{57}\text{Co}$  source (nominal strength 1850 mBq). Low temperature (LT) spectra were collected at 80 K and when necessary at 11 K by using an ARS<sup>®</sup> close-circuit cryostat. The hyperfine parameters isomer shift ( $\delta$ ), quadrupole splitting ( $\Delta$ ), or quadrupole

shift,  $\varepsilon$  when magnetic splitting is present) and full linewidth at half maximum ( $\Gamma$ ), expressed in mm/s, and the internal magnetic field,  $B$ , expressed in T, were obtained by means of a standard least-squares minimisation technique. The spectra were fitted to Lorentzian line shapes using a minimum number of sextets and doublets. We assumed that in all the spectra the hyperfine parameters were affected by the same error, postulated as the maximum error over all the measurements. A variation of  $\pm 0.03$  mm/s with respect to the obtained value is assigned to  $\delta$ ,  $\Delta$  and  $\Gamma$  while  $\pm 2\%$  is assigned to  $A$ . The isomer shift is quoted relatively to metallic iron at room temperature.

The atmosphere in which pottery firing took place can be defined oxidising or reducing on the basis of the so-called “reduction index” (hereafter referred to as R.I.), defined as the ratio of Fe(II) over total Fe [20]. This information can easily be deduced from the Fe(II) area computation in the Mössbauer spectra. The estimation of this parameter was obtained by using the RT values of the relative areas, assuming equal recoilless factors for ferric and ferrous ions. This approximation is not properly correct because the RT measurement involves an overestimation of the ferric component [21]. LT measurements performed on some selected samples showed that by taking into account the experimental errors, the area variation of both ferric and ferrous components did not influence the RT values of R.I. Therefore we assume that the errors calculated by the propagation on the R.I. are larger than the overestimation on the Fe(III) areas and for this reason the RT data for R.I. are considered reliable. In any event LT measurements are necessary in order to recognise oxide nanoparticles, as discussed later.

### 3. Results and discussion

#### 3.1. Chemical, mineralogical and microstructural characterisation

A total of 62 samples of NBPW and BSW were subjected to a complete analytical characterisation. Detailed results can be found in previously published papers [18,19]. In the present work, only some synthetic results are reported, which can be useful for further discussion.

All pastes are non-calcareous (CaO always less than 2% with few exceptions) and show a medium to high iron content (between about 4% and 10%). All samples present a fine microstructure and abundant fine-grained inclusions, and a very simple mineralogy, the only crystalline phases being quartz and variable amounts of illite, besides trace quantities of plagioclase and/or K-feldspars in some cases. The absence of calcium silicates and iron oxides in the diffractograms makes it hard to determine the firing temperature. The presence of illite and its relative abundance, as inferred from XRD patterns, are the only temperature indicators, allowing to estimate the firing temperature in a range between about 850 °C and 950 °C. As far as the atmosphere is concerned, the macroscopic observation of the colour indicates a reducing firing.

The local clayey materials show quite a good chemical correspondence with the archaeological finds. In particular the

finest clays are more similar to the finest samples and vice versa. The observed differences, in terms of chemical composition and granulometric distribution, can be related to the variability of clay deposits, location and time of collection.

The slip layers are characterised by high values of aluminium, iron and potassium/sodium oxides in comparison with the pastes. The hypothesis of the use of local clays subjected only to a refining process has been rejected after laboratory tests. In fact, the purification process alone does not allow one to obtain a product comparable with that used for slips. The quantities of aluminium, iron, potassium and sodium oxides increase but not enough, so an addition of a different product containing these elements to the local clay has been hypothesised [18]. By considering the different quantities of these oxides, three groups of black slips have been identified. A first group shows high amounts of aluminium and iron (AlFe), a second group (KAlFe) was obtained by adding also potassium and sodium, and the last group (Al) is characterised only by high values of aluminium. An addition of the order of 15% for alumina, 5–6% for the iron oxide, and about 1.5% for alkalis can be deduced. Almost all of the BSW slips belong to the AlFe type; this result can be revealing of a specific working technique.

#### 3.2. The Mössbauer spectra

##### 3.2.1. Raw materials

Three selected clays were analysed by using TMS. All three materials are similar from the Mössbauer point of view and are characterised by a strong Fe(III) absorption together with a weak Fe(II) one (about 14% in each sample). The spectra are typical for silicate mixtures whose parameters, reported in Table 1, evidence that iron occupies only octahedral sites. Cooling the system down to 11 K, no magnetic pattern becomes evident. As reported in the literature [22], nanosized iron oxide/oxyhydroxides show a doublet in the RT spectrum, which transforms into a sextet on decreasing the measurement temperature. The temperature at which this transition takes place depends on crystal size, crystallinity, substitution and morphology.

As mentioned above, no real distinction among the clays is possible; nonetheless, the relative amount of Fe(II) can be used as reference to be compared with the R.I. of the archaeological sherds, in order to understand their firing atmosphere.

##### 3.2.2. BSW and NBPW samples

TMS was performed on 15 samples, six of which belonged to the BSW group and the other nine to the NBPW group. The

Table 1  
Mössbauer parameters for RT measurements on clay samples

Sample	$\delta$ (mm/s)	$\Delta$ (mm/s)	$\Gamma$ (mm/s)	$A$ (%)	Attribution
AG160	0.37	0.60	0.44	87	Fe(III) M
	1.11	2.66	0.37	13	Fe(II) M
AG161	0.37	0.65	0.84	86	Fe(III) M
	1.17	2.84	0.71	14	Fe(II) M
AG162	0.35	0.42	0.56	44	Fe(III) M
	0.33	0.99	0.55	42	Fe(III) M
	1.29	2.34	0.57	14	Fe(II) M

M: octahedral site.

Mössbauer parameters are reported in Table 2 and some representative spectra are shown in Fig. 1. All the RT spectra are characterised by strong absorptions due to paramagnetic Fe(III) and Fe(II) species, but the samples may be clustered into three homogeneous groups:

– Group 1 (10 samples): The spectra were fitted by using a four-component model, in which one component is due to octahedral Fe(III), and the other three to Fe(II) species, in octahedral and tetrahedral sites. Both BSW (201, 113/01, 205/01, 10/98, 206/00) and NBPW

Table 2  
Mössbauer parameters for RT measurements on archaeological sherds

Sample	Mössbauer group	Slip group	$\delta$ (mm/s)	$\Delta$ (mm/s)	$\Gamma$ (mm/s)	A (%)	R.I.	Attribution
BSW201	1	AlFe	0.43	0.81	0.71	25	0.75	Fe(III) M
			1.07	2.54	0.58	31		Fe(II) M
			0.99	1.96	0.64	33		Fe(II) T
			0.88	1.28	0.52	11		Fe(II) H
BSW113/01	1	AlFe	0.44	0.98	0.48	18	0.82	Fe(III) M
			1.17	2.41	0.40	18		Fe(II) M
			1.02	2.00	0.52	26		Fe(II) T
			0.87	1.25	0.76	38		Fe(II) H
BSW207	2	KAlFe	0.43	0.91	0.84	41	0.59	Fe(III) M
			1.08	2.48	0.52	37		Fe(II) M
			1.04	1.93	0.46	22		Fe(II) T
BSW205/01	1	AlFe	0.32	0.87	0.57	16	0.84	Fe(III) M
			1.15	2.52	0.48	23		Fe(II) M
			1.00	1.93	0.54	23		Fe(II) T
			0.91	1.23	0.70	38		Fe(II) H
BSW10/98	1	AlFe	0.28	1.06	0.62	54	0.46	Fe(III) M
			1.04	2.31	0.39	14		Fe(II) M
			0.99	1.97	0.43	14		Fe(II) T
			0.75	1.27	0.86	19		Fe(II) H
BSW206/00	1	Al	0.36	0.85	0.52	21	0.79	Fe(III) M
			1.05	2.64	0.50	33		Fe(II) M
			1.07	1.99	0.57	25		Fe(II) T
			0.63	1.29	0.68	21		Fe(II) H
NBPW22/00	2	KAlFe	0.33	0.76	0.69	34	0.66	Fe(III) M
			1.07	2.60	0.58	17		Fe(II) M
			0.93	1.69	0.89	49		Fe(II) T
NBPW18/00	1	KAlFe	0.37	0.75	0.61	32	0.68	Fe(III) M
			1.09	2.61	0.41	19		Fe(II) M
			1.01	2.07	0.49	23		Fe(II) M
			0.88	1.42	0.70	26		Fe(II) H
NBPW8/98	1	KAlFe	0.28	0.92	0.50	36	0.64	Fe(III) M
			1.13	2.30	0.46	25		Fe(II) M
			0.99	1.91	0.50	16		Fe(II) T
			0.87	1.29	0.69	23		Fe(II) H
NBPW6/00	1	KAlFe	0.39	0.72	0.65	34	0.66	Fe(III) M
			1.07	2.47	0.41	23		Fe(II) M
			1.06	2.03	0.28	10		Fe(II) M
			0.87	1.55	0.84	33		Fe(II) H
NBPW5/98	1	AlFe	0.33	0.76	0.66	21	0.79	Fe(III) M
			1.10	2.60	0.40	16		Fe(II) M
			1.04	1.94	0.54	40		Fe(II) T
			0.89	1.32	0.69	28		Fe(II) H
NBPW13/98	1	AlFe	0.29	0.95	0.66	38	0.62	Fe(III) M
			1.13	2.42	0.39	18		Fe(II) M
			1.05	1.96	0.49	21		Fe(II) T
			0.87	1.40	0.77	23		Fe(II) H
NBPW11/98	2	Al	0.36	0.83	0.62	84	0.1	Fe(III) M
			1.06	2.66	0.34	7		Fe(II) M
			1.08	1.98	0.33	9		Fe(II) T
NBPW1/98	3	KAlFe	0.34	0.55	0.43	41	0.27	Fe(III) M
			0.42	1.02	0.54	34		Fe(III) M
			1.12	2.47	0.56	27		Fe(II) M
NBPW7/98	3	Al	0.33	0.78	0.42	38	0.08	Fe(III) M
			0.34	1.40	0.66	54		Fe(III) M
			1.00	1.92	0.65	8		Fe(II) T

Groupings made on the base of Mössbauer data and of slip chemistry are indicated. M: octahedral site; T: tetrahedral site; H: hercynite; R.I.: reduction index. The  $\delta$  values are relative to metallic  $\alpha$ -iron.

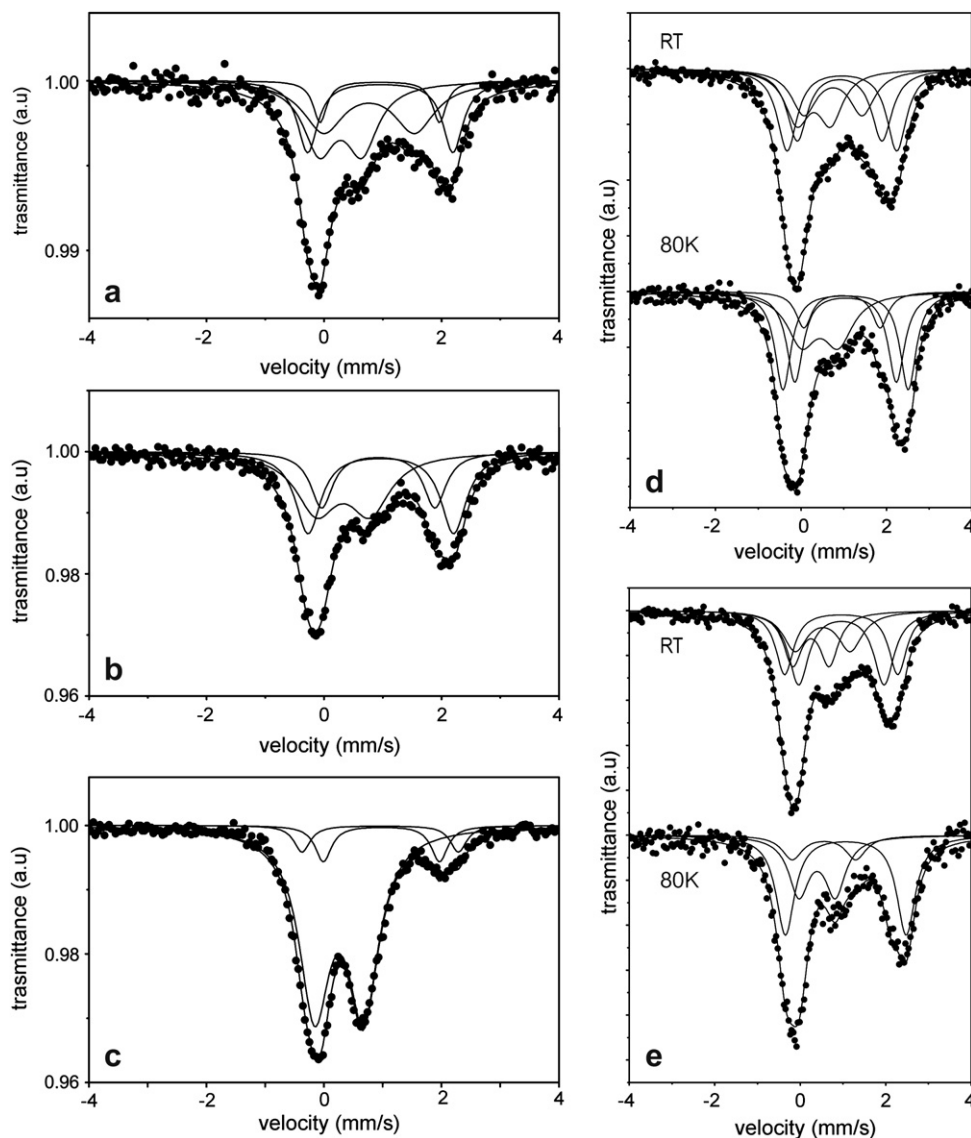


Fig. 1. Room temperature (RT) and low temperature (80 K) Mössbauer spectra of selected BSW and NBPW samples. (a) RT spectrum of NBPW 6/00. (b) RT spectrum of BSW 207. (c) RT spectrum of NBPW 11/98. (d) RT and 80 K spectra of BSW 201. (e) RT and 80 K spectra of BSW 206.

samples (18/00, 8/98, 6/00, 5/98, 13/98) belong to this group.

- Group 2 (3 samples): The spectra were fitted by using a three-component model, in which one component is due to octahedral Fe(III), and the other two to octahedral and tetrahedral Fe(II). Samples BSW207, NBPW22/00 and NBPW11/98 belong to this group.
- Group 3 (2 samples): The spectra were fitted by using a three-component model, in which two components are due to octahedral Fe(III) and one to either octahedral or tetrahedral Fe(II). Samples NBPW1/98 and NBPW7/98 belong to this group.

The absorption due to Fe(II) species is composed by the superimposition of several components attributable to tetrahedral and octahedral sites, with parameters typical of hercynite (in group 1) and spinel (in groups 1 and 2). A doublet due to

octahedral Fe(II), that can be assigned to Fe(II) borne in neo-genesis phases, silicate minerals and/or amorphous phases, is always present. The presence of spinel and/or hercynite is associated with a high firing temperature (above 900 °C) and with a reducing atmosphere [23]. This result is in agreement with the hypothesis of a firing at 900–950 °C, made on the basis of previous analyses [18,19]. The ferric components of both groups 1 and 2 present parameters typical of Fe(III) borne in silicate minerals. The rather large  $\Delta$  values could suggest the presence of nanosized Fe oxide [22]. LT spectra were therefore collected on some selected samples (cf. Fig. 1d and e, and Table 3) but no evidence of magnetic patterns or relaxation components was detected. As no oxide is present, and due to the high firing temperature, the broad linewidth can be related to the presence of Fe(III) in the amorphous matrix. Fe(III) borne in such a disordered system can in fact give rise to a broad doublet, characterised not only by a large  $\Gamma$ , but

Table 3  
Mössbauer parameters for 80 K measurements of selected archaeological samples

Sample	$\delta$ (mm/s)	$\Delta$ (mm/s)	$\Gamma$ (mm/s)	A (%)	Attribution
BSW201	0.55	0.86	0.84	28	Fe(III) M
	1.20	2.38	0.46	29	Fe(II) M
	1.19	2.93	0.45	31	Fe(II) M
	1.07	1.79	0.45	11	Fe(II) H
BSW206/00	0.49	0.89	0.81	39	Fe(III) M
	1.18	2.83	0.44	22	Fe(II) M
	1.17	2.15	0.44	27	Fe(II) T
	0.73	1.37	0.39	10	Fe(II) H
BSW207/00	0.43	0.92	0.90	46	Fe(III) M
	1.22	2.74	0.48	32	Fe(II) M
	1.19	2.11	0.44	22	Fe(II) T

M: octahedral site; T: tetrahedral site; H: hercynite. The  $\delta$  values are relative to metallic  $\alpha$ -iron.

also by a large  $\Delta$ . This high value is to be ascribed to a lack of symmetry in the electric field gradient on the Fe(III) nucleus, probably due to structural disorder.

Samples belonging to group 3 are completely different from the other ones. As is evident from the RT spectra (Fig. 2) and Mössbauer parameters (Table 4), the amount of ferric component is considerably larger than in the other groups. The spectra of these samples can be well fitted only by using a model with two ferric components, differing from each other for the value of  $\Delta$ . The site with the largest  $\Delta$  (1.02 mm/s in NBPW1/98 and 1.40 mm/s in NBPW7/98) is probably linked to the presence of nanosized iron oxide particles. In fact, the LT spectra of both samples do show a magnetic pattern. The spectrum of NBPW7/98 is already magnetically ordered at 80 K and the parameters are typical of haematite with an average particle size that could be estimated at about 10 nm [22]. Measurements at 11 K show that the increase of the sextet relative area is negligible, as well as the variation on the ferric site parameters. This is due to the overlapping of two ferric sites that cannot be resolved for the different temperature dependence. The absorption with the highest quadrupole splitting in the RT spectrum is therefore due to the superimposition of a ferric ion present in the silicate structure and of the nanosized iron oxide. The low percentage of Fe(II) and the presence of haematite suggest that this sample was fired under oxidising conditions.

Differently from NBPW7/98, sample NBPW1/98 shows a magnetically ordered spectrum at 11 K with an  $\epsilon$  value close to 0 and a small internal field, parameters that could indicate the presence of nanosized maghemite,  $\gamma$ -Fe<sub>2</sub>O<sub>3</sub>. The broad linewidth could be due to a low crystallinity of this oxide. The discussion concerning the paramagnetic area variations as a function of the measurement temperature is valid also for this sample. The presence of maghemite together with a not negligible percentage of Fe(II) may be in agreement with a variation of the atmosphere during firing. A reducing atmosphere could in fact promote, above a certain temperature, the formation of Fe(II) bearing oxides, such as spinels, and a subsequent variation in the O<sub>2</sub> fugacity towards an oxidising atmosphere, such as that due to a kiln opening, could promote the formation of maghemite.

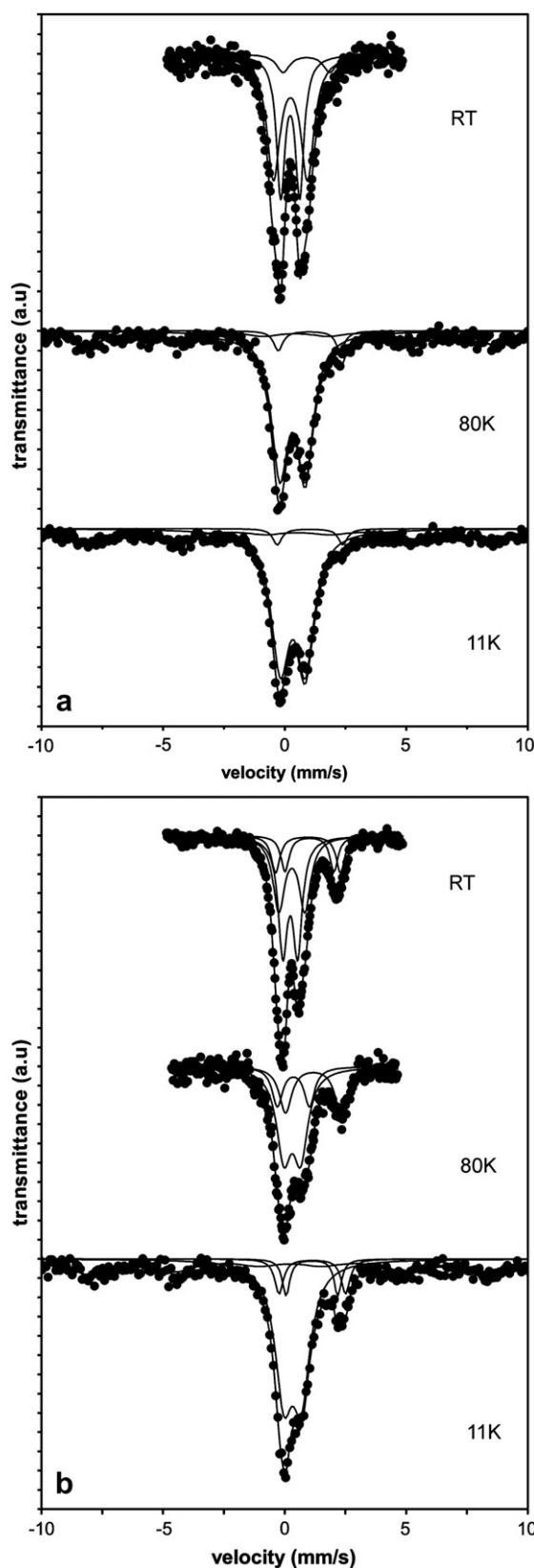


Fig. 2. Top to bottom: RT, 80 K and 11 K spectra of (a) NBPW7/98 and (b) NBPW1/98.

Table 4  
Mössbauer parameters for RT and LT (80 K and 11 K) measurements on group 3 samples

Sample	Temp. (K)	$\delta$ (mm/s)	$\Delta$ ( $\epsilon$ ) (mm/s)	$\Gamma$ (mm/s)	$B$ (T)	$A$ (%)	Attribution
NBPW7/98	298	0.33	0.78	0.42		38	Fe(III) M
		0.34	1.40	0.66		54	Fe(III) M
		1.00	1.92	0.65		8	Fe (II) T
	80	0.43	1.04	0.89		68	Fe(III) M
		0.47	-0.15	1.90	51.8	26	Hem.
		1.11	2.55	0.45		6	Fe(II) T
	11	0.41	1.03	0.81		66	Fe(III) M
		0.53	-0.22	1.57	52.0	30	Hem.
		1.15	2.69	0.44		4	Fe(II) T
NBPW1/98	298	0.34	0.55	0.43		41	Fe(III) M
		0.42	1.02	0.54		34	Fe(III) M
		1.12	2.47	0.56		27	Fe(II) M
	80	0.41	0.68	0.72		55	Fe(III) M
		0.46	1.31	0.52		19	Fe(III) M
		1.29	2.28	0.61		26	Fe(II) M
	11	0.42	0.73	0.78		40	Fe(III) M
		0.43	0.05	2.45	50.9	40	Hem./Magh.
		1.25	2.38	0.84		20	Fe(II) M

M: octahedral site; T: tetrahedral site; Hem: haematite; Magh: maghemite. The  $\delta$  values are relative to metallic  $\alpha$ -iron.

### 3.3. The reduction index (R.I.)

As shown in Fig. 3, the R.I. values of the two groups (BSW and NBPW) are quite high; all BSW samples present R.I. values greater than 0.35, while all the values for NBPW samples fall inside the range 0.08–0.84. The value of 0.20, plotted as a dotted line in the graphs, represents the upper limit of the amount of Fe(II) in the analysed clays. In order to identify possible clustering between the two populations, R.I. values have been plotted versus themselves, but, as evident in Fig. 3b, it is still not possible to distinguish between BSW and NBPW samples. However, it can be observed that R.I. values seem to have some relationship with a different partitioning of the samples, made accordingly to the EDS chemical analysis of the slips. As already mentioned, chemical data have pointed out the existence of three types of slips, and the samples have consequently been grouped as indicated in Table 2. If we now use this criterion to identify samples in the R.I. plot (Fig. 3b), some interesting comments can be proposed. First of all, KAlFe-group samples do form a group in this graph, with the exception of sample NBPW1/98, which by the way shows peculiar features even on a macroscopic scale. The limited variability of R.I. values for these samples seems to suggest a highly controlled firing cycle, especially as far as the firing atmosphere is concerned. On the other hand, AlFe-group samples and even more so those of the Al-group are widely spread on the graph, which seems to indicate a less effective control on the firing process by the potter.

## 4. Conclusions

The use of Mössbauer spectroscopy for the analysis of Nepalese black slipped pottery showed once again how this

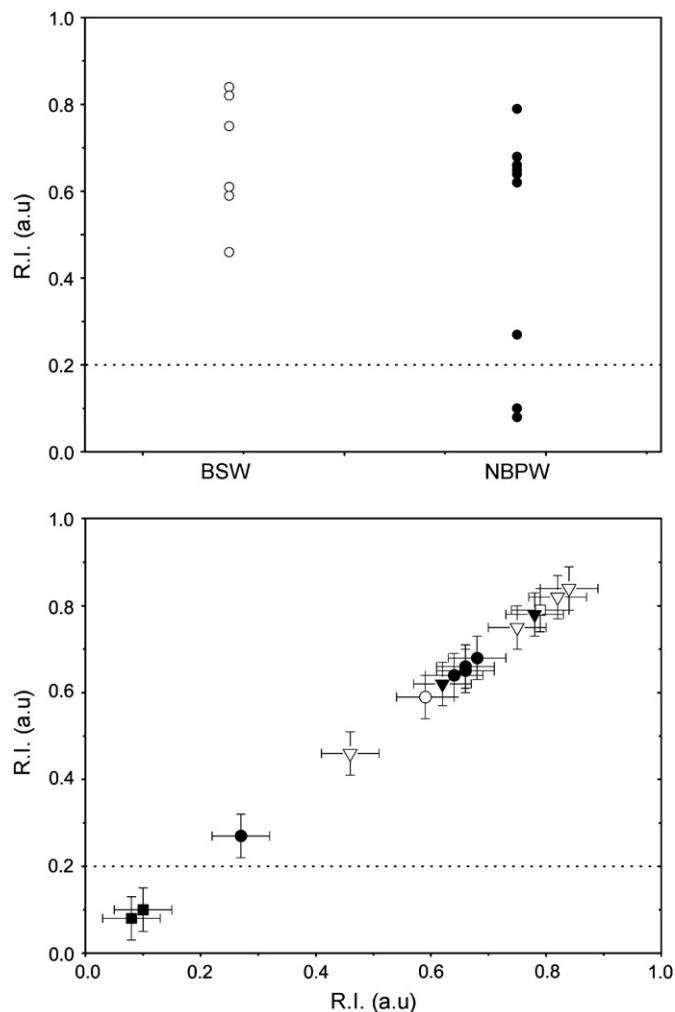


Fig. 3. (a) Distribution of R.I. as function of the ceramic class. (b) R.I. vs. itself; closed symbols for NBPW, open symbols for BSW; circle for KAlFe group, square for Al group and triangle for AlFe group. Error bars for both  $x$  and  $y$  values are plotted in the graph.

technique can be a valuable support to routine analytical methodologies, when additional information about the firing process is needed. Chemical, mineralogical and microstructural analyses pointed out the difficulty in clearly distinguishing BSW and NBPW on an analytical basis, as in determining the firing technique used by the potter. Mössbauer data did not solve the classification question, but allowed definition with a greater level of confidence of the temperature interval in which the artefacts were fired, which ranges between 900 °C and 950 °C. Clustering the samples by different fitting models allowed one to discriminate those fired in a well-controlled, non-oxidising atmosphere from those fired in a not so well-controlled atmosphere. In fact, as mentioned in Section 3.2.2, the presence of maghemite in group 3 samples could be ascribed to a variation in the kiln atmosphere.

The computation of the reduction index also allowed to hypothesise the existence of a relationship between the chemical composition of the three slip groups and the production technology of the artefacts, especially regarding the more or

less accurate control of the firing atmosphere by the potter. This hypothesis will be the starting point for a future work involving nuclear techniques such as neutron activation and/or PIXE-PIGE spectrometry. By using these investigatory tools a deep and complete elemental analysis could be performed, underlining the relationship mentioned above. This is an interesting though preliminary result, not only because it establishes a link between archaeometric analyses made on the slips and on the pastes of the same samples. In fact, it also produces feedback towards the archaeological research, stimulating it in the direction of a renewed and different classification of the materials, on the basis of the global results of the archaeometric study.

## References

- [1] L. Nodari, L. Maritan, C. Mazzoli, U. Russo, Sandwich structures in the Etruscan-Padan type pottery, *Appl. Clay Sci.* 27 (2004) 119–128.
- [2] L. Stievano, M. Bertelle, B. Fabbri, S. Calogero,  $^{57}\text{Fe}$  Mössbauer study of the firing temperature of Renaissance ceramics from Faenza, *Sci. Tech. Cult. Herit.* 5 (1996) 37–46.
- [3] M. Bertelle, S. Calogero, M. Oddone, R. Salerno, R. Segnan, L. Stievano, Firing techniques of the impasti from the protohistoric site of Concordia Sagittaria (Venice), *J. Cult. Herit.* 1 (2000) 261–279.
- [4] N.H. Gangas, A. Kostikas, A. Simopoulos, J. Vocotopoulou, Mössbauer spectroscopy of Ancient Greek pottery, *Nature* 229 (1971) 485–486.
- [5] U. Wagner, R. Gebhard, G. Grosse, T. Hutzelman, E. Murad, J. Riederer, I. Shimada, F.E. Wagner, Clay: An important raw material for prehistoric man, *Hyperfine Interact.* 117 (1998) 323–335.
- [6] F.E. Wagner, U. Wagner, Mössbauer spectra of clays and ceramics, *Hyperfine Interact.* 154 (2004) 35–82.
- [7] M. Maggetti, Phase analysis and its significance for technology and origin, in: J. Olin, A.D. Franklin (Eds.), *Archaeological Ceramics*, Smithsonian Institution Press, Washington DC, 1982, pp. 121–133.
- [8] A. Livingstone Smith, Bonfire II: the return of pottery firing temperatures, *J. Archaeol. Sci.* 28 (2001) 991–1003.
- [9] S. Wolf, Estimation of the production parameters of very large medieval bricks from St. Urban, Switzerland, *Archaeometry* 44 (2002) 37–65.
- [10] B. Fabbri, The problem of defining the firing temperature of ceramic artefacts, in: C. Ariao, A. Bietti, L. Castelletti, C. Peretto (Eds.), *Proceedings of the XIII UISPP Congress, Forlì, Sept. Vol. I, A.B.A.C.O., Forlì, 1996–1998*, pp. 8–14.
- [11] M.M. Fernandez, J. Buxeda, I. Garrigos, A review of the archaeometric studies of western Mediterranean *terra sigillata* from the first century B.C. to the second century A.D.: state of art, limitations and potential, in: V. Kilikoglou, A. Hein, Y. Maniatis (Eds.), *Modern trends in scientific studies on ancient ceramics—Bar Int. series 1011*, Proceedings of the 5th EMAC, Athens, Greece, 1999, Archaeopress, Oxford, UK, 2002, pp. 287–298.
- [12] P. Duminuco, M.P. Ricciardi, B. Messiga, M. Setti, Modificazioni tessurali e mineralogiche come indicatori della dinamica del processo di cottura di manufatti ceramici, *Ceramurgia* 26 (1996) 281–288.
- [13] A. Moropoulou, A. Bakolas, K. Bisbikou, Thermal analysis as a method of characterizing ancient ceramic technologies, *Thermochim. Acta* 2570 (1995) 743–753.
- [14] P. Mirti, P. Davit, New development in the study of ancient pottery by colour measurements, *J. Archaeol. Sci.* 31 (2004) 741–751.
- [15] G. Verardi, Excavations at Gotihawa and a territorial survey in Kapilavastu District of Nepal. A preliminary report, *Lumbini International Research Institute Occasional Papers* 2, 2002.
- [16] G. Verardi, Excavations at Gotihawa and Pipri, *Kapilbastu Distric, Nepal, Rome* (forthcoming).
- [17] M.I. Panaccione Apa, A.A. Di Castro, A preliminary classification and chronological sequence of Gotihawa Pottery, in: M. Taddei, G. De Marco (Eds.), *South Asian Archaeology 1997*, Vol. 3, Istituto Italiano per l’Africa e l’Oriente, Roma, 2000, pp. 717–737.
- [18] L. Camarda, E. Cerchi, B. Fabbri, S. Gualtieri, G. Verardi, Scientific investigation and classification of nepalese slipped pottery from Gotihawa (Nepalese Tarai), in: S. Di Pierro, V. Serneels, M. Maggetti (Eds.), *Ceramics in the Society*, Proceedings of the 6th EMAC, Fribourg, Switzerland, 3–6 October 2001, Department of Geosciences Mineralogy and Petrography, Fribourg, 2003, pp. 51–63.
- [19] L. Camarda, E. Cerchi, B. Fabbri, S. Gualtieri, G. Verardi, Classification and typology of the pottery from Gotihawa (Nepalese Tarai), with particular reference to the NBPW, in: C. Jarrige, V. Lefevre (Eds.), *South Asian Archaeology 2001*, Vol. I (Prehistory), Editions Recherche sur les Civilisations ADPF, Paris, 2005, pp. 35–49.
- [20] M. Maggetti, G. Galetti, Archäometrische Untersuchungen an spätlateinzeitlicher Keramik von Basel-Gasfabrik und Sissach-Brühl, *Archäologisches Korrespondenzblatt* 11 (1981) 321–328.
- [21] E. De Grave, A. Van Alboom, Evaluation of ferrous and ferric Mössbauer fractions, *Phys. Chem. Miner.* 18 (1991) 337–342.
- [22] E. Murad, J.H. Johnston, Iron oxides and hydroxides, in: G.J. Long (Ed.), *Mössbauer Spectroscopy Applied to Inorganic Chemistry*, Vol. 2, Plenum Press, New York, 1987.
- [23] L. Maritan, L. Nodari, C. Mazzoli, U. Russo, Grey pottery from Este (North eastern Italy): provenance and production technology, *Appl. Clay Sci.* 29 (1) (2005) 31–44.